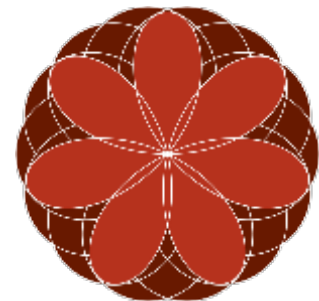


Laboratory measured stress dependence in shales at seismic and ultrasonic frequencies

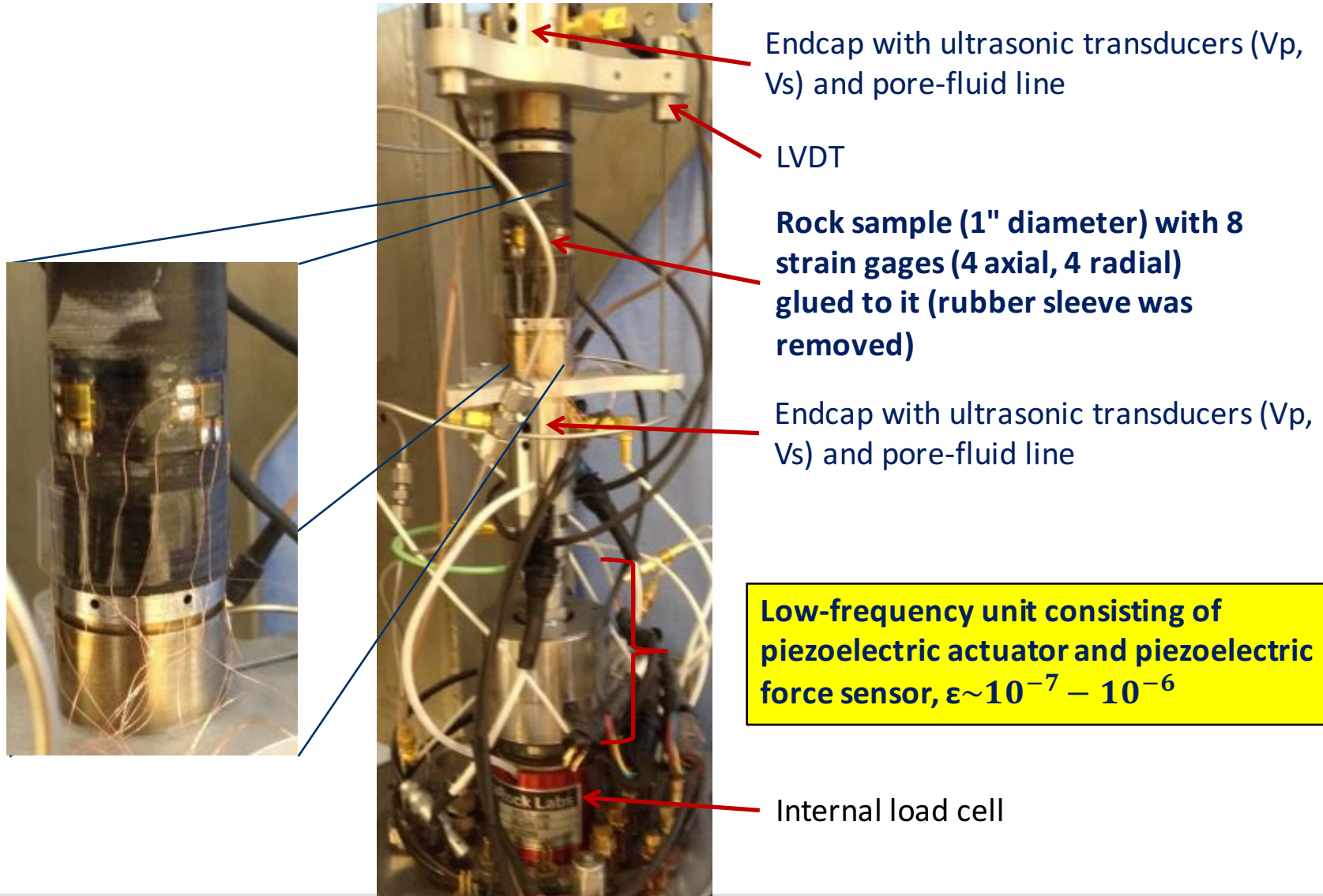
by

Dawid Szewczyk, Andreas Bauer, Rune M. Holt

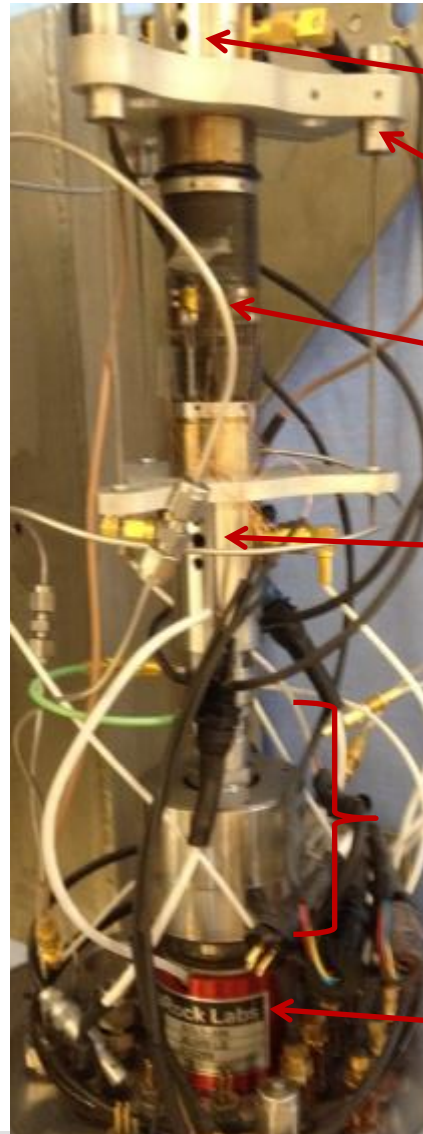
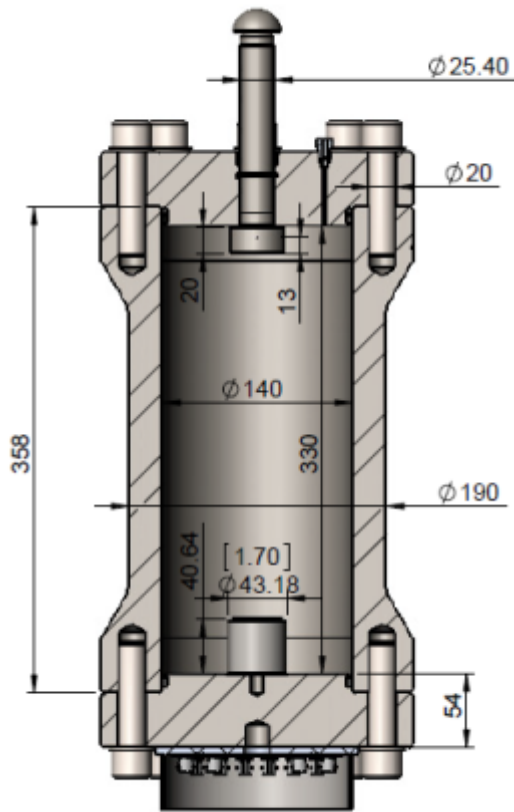
ROSE meeting
25th - 28th April 2016
Trondheim, Norway



Biaxial cell for seismic-dispersion measurements



Biaxial cell for seismic-dispersion measurements



Endcap with ultrasonic transducers (V_p , V_s) and pore-fluid line

LVDT

Rock sample (1" diameter) with 8 strain gages (4 axial, 4 radial) glued to it (rubber sleeve was removed)

Endcap with ultrasonic transducers (V_p , V_s) and pore-fluid line

Low-frequency unit consisting of piezoelectric actuator and piezoelectric force sensor, $\epsilon \sim 10^{-7} - 10^{-6}$

Internal load cell

Stress dependence – Sample preparation

Mancos shale: outcrop, gas shale, preserved in oil, density 2.57 g/cm^3 , 1-11% porosity, 20-25% clay, 40-50% quartz, 1% -1,5% TOC, tested in as-received conditions

Pierre shale: outcrop material preserved in oil, density 2.40 g/cm^3 , 10-25% porosity, 40-80% clay, 5-25% quartz, saturation levels tuned

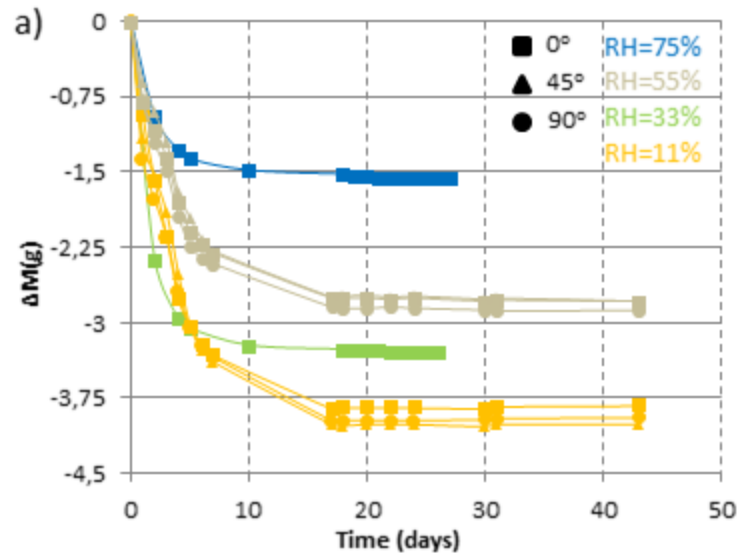
Expose samples to different relative humidity [RH]

11.3% [LiCl]

32.9% [MgCl]

54,7% [Mg(NO₃)₂]

75.4% [NaCl]



- RH control → saturated solutions of different type of salts
- RH → saturated conversion: mineral density + XRD composition → ρ_T (0 porosity); $\rho_T + \rho_M(\text{measured}) \rightarrow \phi$; $\phi + V_S \rightarrow V_\phi$; $V_\phi + \Delta M \rightarrow S_W$

Stress dependence – Data processing

Seismic frequencies → Rock engineering parameters (E, ν)

Ultrasonic frequencies → P- and S-wave velocities

Conversion

Isotropic materials:

$$E_{Isot} = \frac{\rho V_S^2 (3V_P^2 - 4V_S^2)}{V_P^2 - V_S^2}$$

$$\nu_{Isot} = \frac{V_P^2 - 2V_S^2}{2(C_{V_P^2} - V_S^2)}$$

TI medium:

$$E_{V-Anisot} = C_{33} - \frac{C_{13}^2}{(C_{11} - C_{66})}$$

$$\nu_{VH-Anisot} = \frac{C_{13}}{2(C_{11} - C_{66})}$$

$$C_{33} = \rho V_{PV}^2, \quad C_{44} = \rho V_{SV}^2, \quad C_{11} = \rho V_{PH}^2, \quad C_{66} = \rho V_{SH}^2$$

$$C_{13} = \frac{\sqrt{(2\rho V_{qP}^2 - \rho V_{PH}^2 \sin^2 \theta - \rho V_{PV}^2 \cos^2 \theta - \rho V_{SV}^2)^2 - ((\rho V_{PH}^2 - \rho V_{SH}^2) \sin^2 \theta - (\rho V_{PV}^2 - \rho V_{SV}^2) \cos^2 \theta)^2}}{2 \sin \theta \cos \theta} - \rho V_{SV}^2$$



Stress dependence – Data processing

# of sample	Shale	Orientation with respect to bedding	Saturant	RH theoretical (RH measured in the day of experiment)	Saturation	Change of volume during stabilization (%)
S 01, 02, 03	Mancos "B"	0°, 45°, 90°	As received	- (~86%)	~ 0.71	0
S 04, 05, 06	Pierre	0°, 45°, 90°	LiCl	11.3% (18.9%)	~ 0.12	~ -3 ÷ -4
S 07	Pierre	0°	MgCl ₂	32.9% (33.9%)	~ 0.27	-3,10
S 08, 09, 10	Pierre	0°, 45°, 90°	Mg(NO ₃) ₂	54.4% (55.1%)	~ 0.50	~ -2,5 ÷ -3,2
S 11	Pierre	0°	NaCl	75.4% (76%)	~ 0.72	-3,16

Vertical properties + Thomsen parameters → Elastic coefficients (C_{ij})

$$C_{11} = \frac{E_V(v_{VH} - 1)}{(v_{VH} + 1)(2v_{VH} - 1)} - \frac{2E_V(v_{VH} - 1)(2v_{VH}^2 - v_{VH} + 1)}{(v_{VH} + 1)^2(2v_{VH} - 1)^2} \varepsilon + \frac{4v_{VH}^2 E_V}{(v_{VH} + 1)^2(2v_{VH} - 1)} \gamma + \frac{2v_{VH}^2 E_V(v_{VH} - 1)}{(v_{VH} + 1)^2(2v_{VH} - 1)^2} \delta$$

$$C_{33} = \frac{E_V(v_{VH} - 1)}{(v_{VH} + 1)(2v_{VH} - 1)} - \frac{8v_{VH}^2 E_V(v_{VH} - 1)}{(v_{VH} + 1)^2(2v_{VH} - 1)^2} \varepsilon + \frac{4v_{VH}^2 E_V}{(v_{VH} + 1)^2(2v_{VH} - 1)} \gamma + \frac{2v_{VH}^2 E_V(v_{VH} - 1)}{(v_{VH} + 1)^2(2v_{VH} - 1)^2} \delta$$

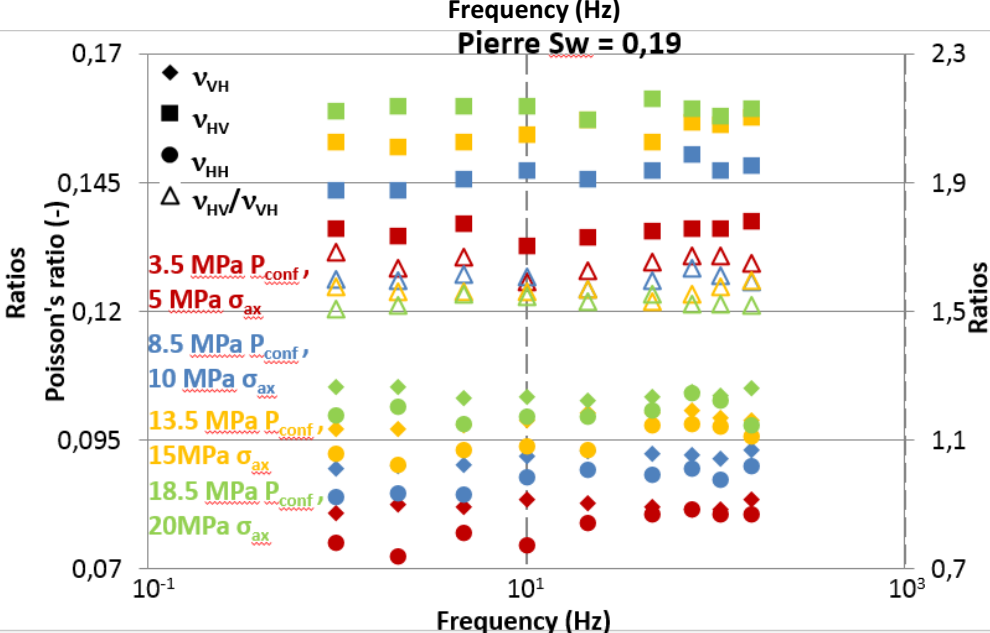
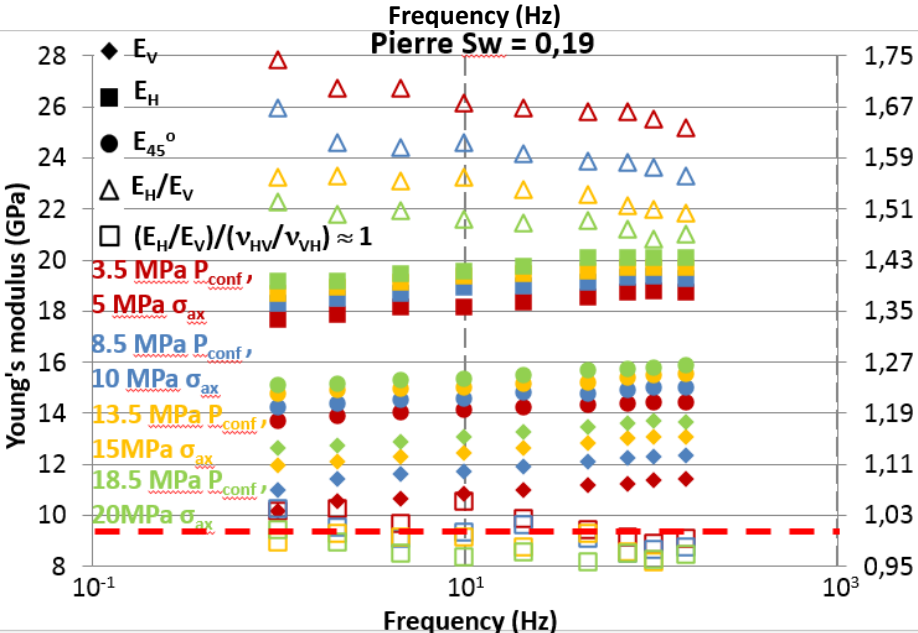
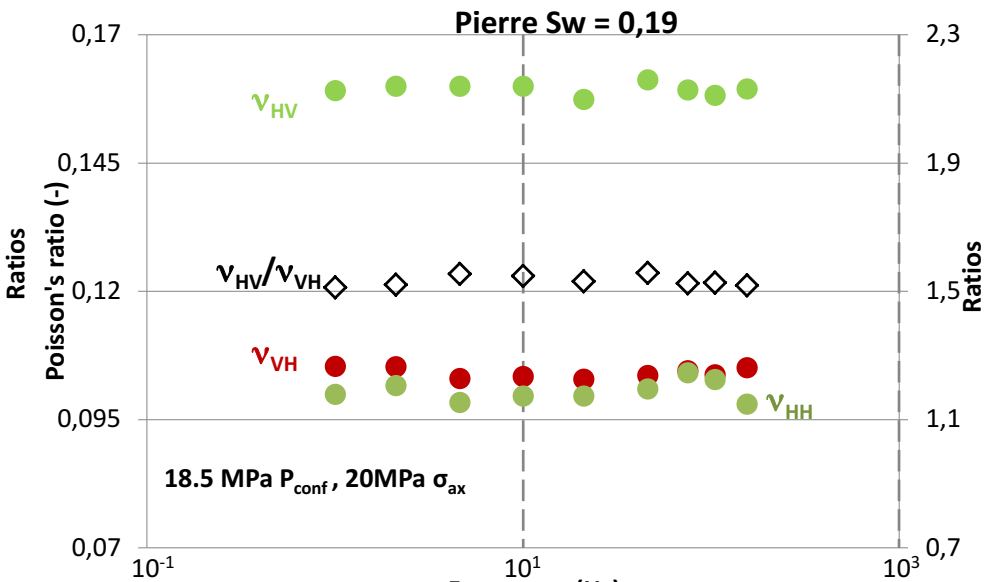
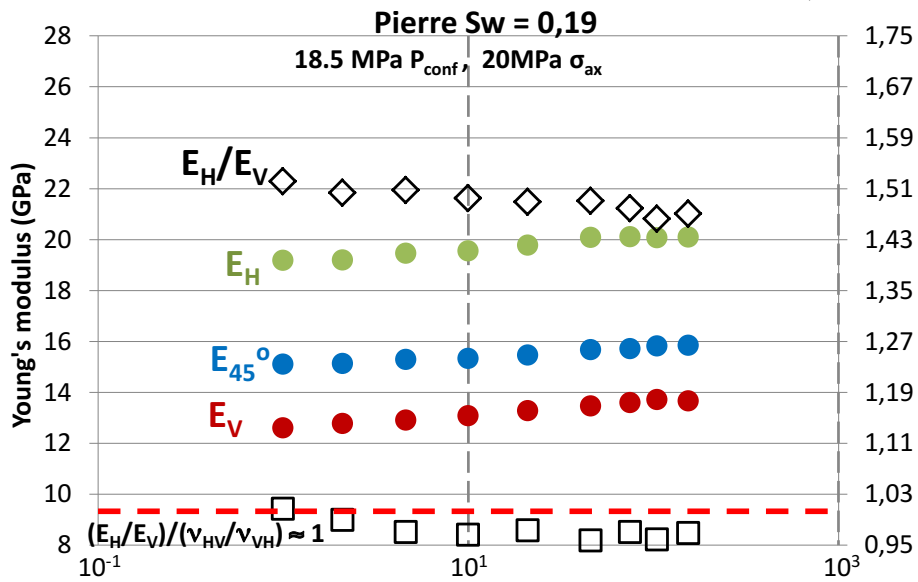
$$C_{44} = \frac{E_V}{2(v_{VH} + 1)} + \frac{2v_{VH} E_V(v_{VH} - 1)}{(v_{VH} + 1)^2(1 - 2v_{VH})} \varepsilon + \frac{v_{VH} E_V}{(v_{VH} + 1)^2} \gamma - \frac{(v_{VH} - 1)(2v_{VH} + 1) E_V}{2(v_{VH} + 1)^2(1 - 2v_{VH})} \delta$$

$$C_{66} = \frac{E_V}{2(v_{VH} + 1)} + \frac{2v_{VH} E_V(v_{VH} - 1)}{(v_{VH} + 1)^2(1 - 2v_{VH})} \varepsilon + \frac{E_V(2v_{VH} + 1)}{(v_{VH} + 1)^2} \gamma - \frac{(v_{VH} - 1)(2v_{VH} + 1) E_V}{2(v_{VH} + 1)^2(1 - 2v_{VH})} \delta$$

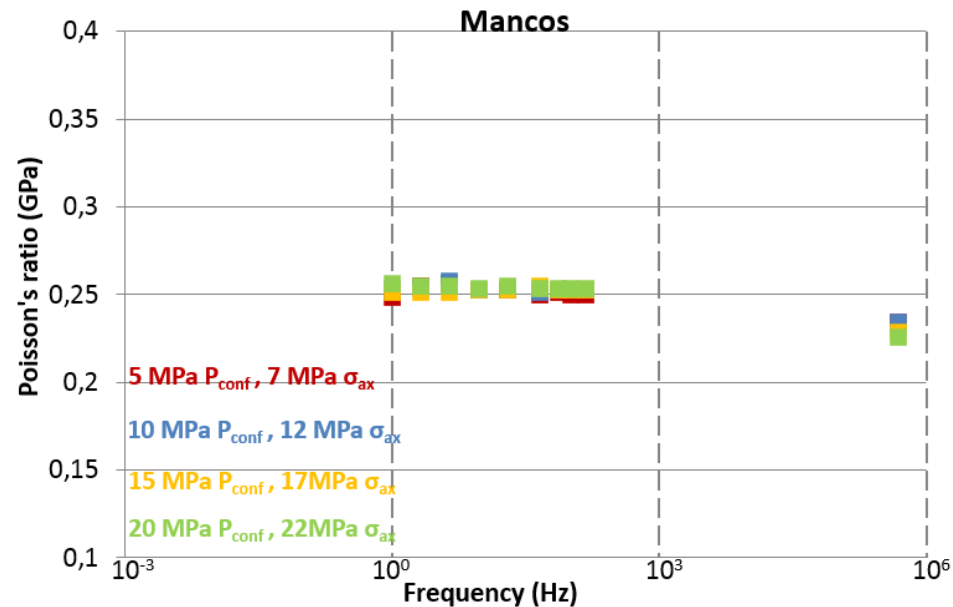
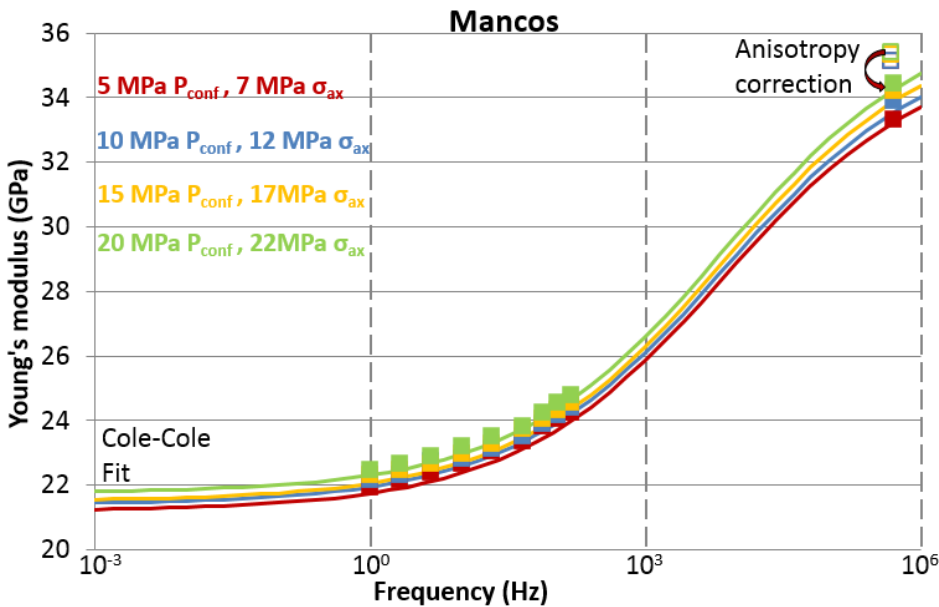
$$C_{13} = \frac{-E_V v_{VH}}{(v_{VH} + 1)(2v_{VH} - 1)} - \frac{4v_{VH} E_V(v_{VH} - 1)}{(v_{VH} + 1)^2(2v_{VH} - 1)^2} \varepsilon + \frac{2v_{VH} E_V}{(2v_{VH} - 1)(v_{VH} + 1)^2} \gamma + \frac{v_{VH} E_V(v_{VH} - 1)}{(v_{VH} + 1)^2(2v_{VH} - 1)^2} \delta$$

Stress dependence – Quality check

➤ TI symmetry requires: $\frac{\nu_{HV}}{E_H} = \frac{\nu_{VH}}{E_V}$

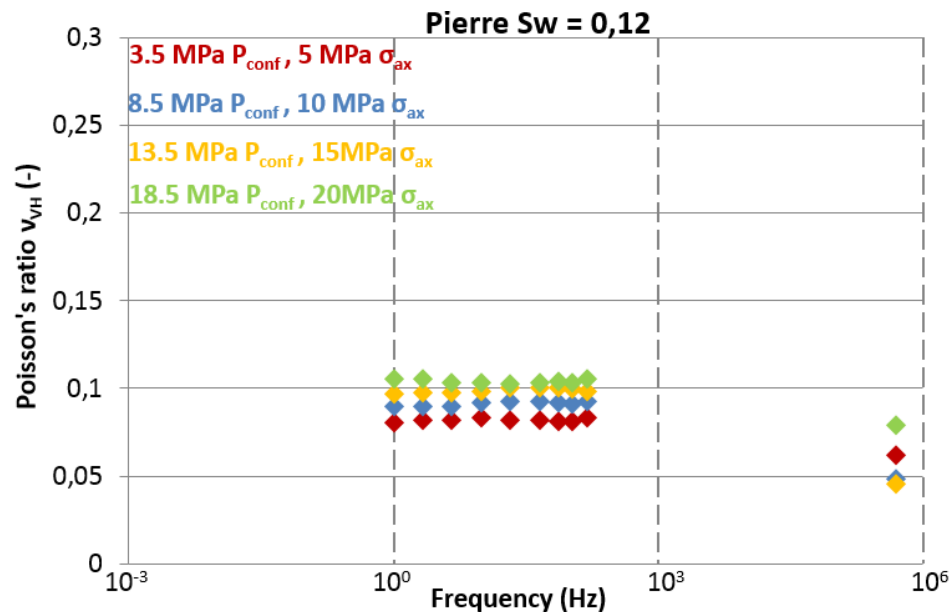
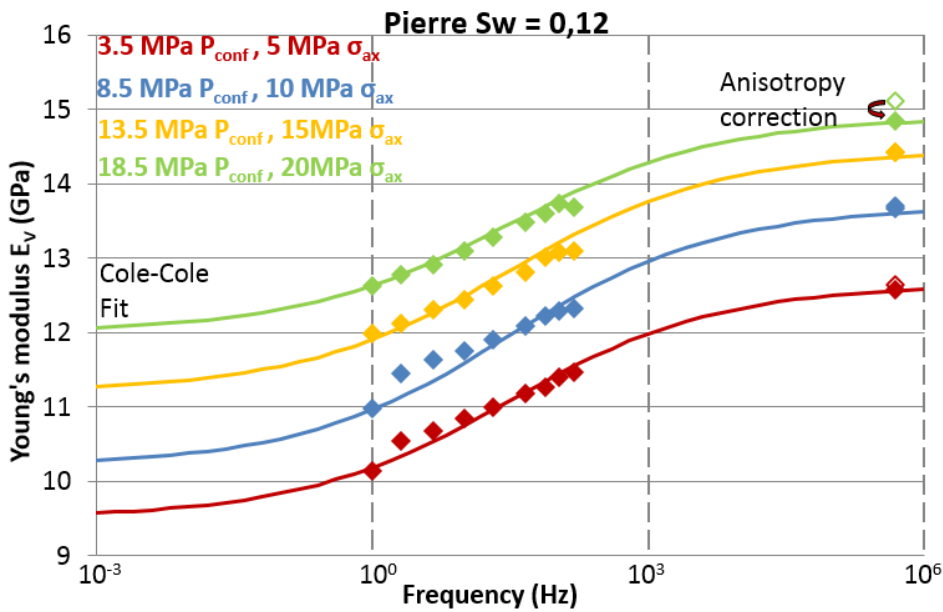


Stress dependence – E_V - Mancos shale



- Dispersion → ~ 50% in E_V (~ 10% at seismic frequencies)
- Stress sensitivity ~ 0.15%/MPa
- Absolute E_V changes similar at seismic and ultrasonic frequencies (relative changes are higher at seismic frequencies due to dispersion)
- Poisson's ratio non-dispersive at seismic frequencies and rather stress independent

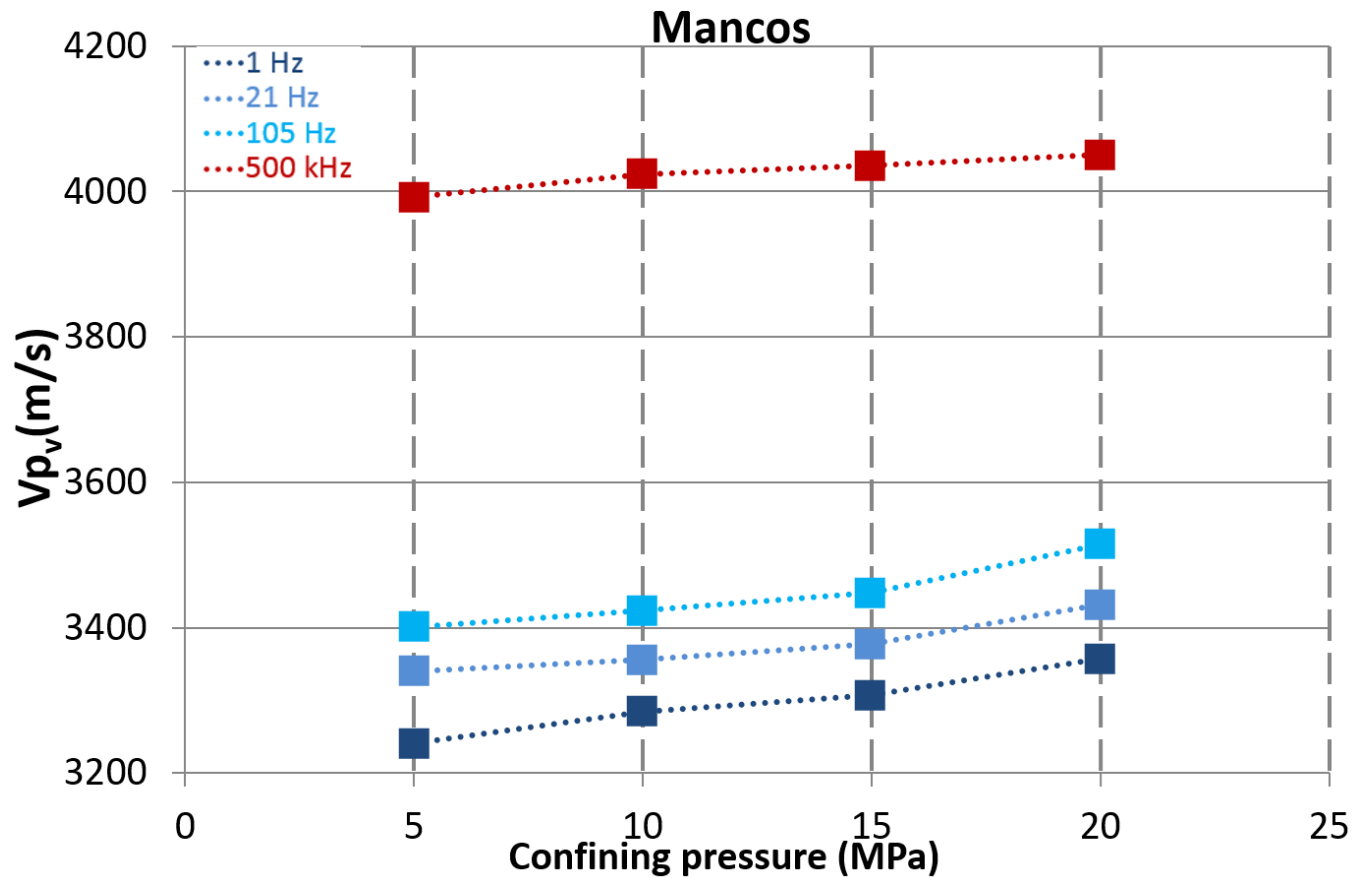
Stress dependence – E_V - Pierre shale



- Dispersion \rightarrow $\sim 24\%$ in E_V at low stresses and $\sim 17\%$ at high stresses (increases with increasing S_w)
- Stress sensitivity $\sim 1.6\%/MPa$ and decreases with increasing saturation ($0.7\%/MPa$ for $S_w=0.72$)
- Absolute E_V changes similar at seismic and ultrasonic frequencies (relative changes are smaller at ultrasonic frequencies due to dispersion)
- Poisson's ratio \rightarrow non-dispersive at seismic frequencies (from $S_w=0.5$ some dispersion may be observed), clear stress dependency

Stress dependence – V_{pV} -Mancos shale

Frequency (Hz)	Stress sensitivity (m/s/MPa)
1	7.45
21	7.38
105	7.29
500 k	3.7



- Stress sensitivity → clear difference between seismic and ultrasonic frequencies (~ twofold higher at seismic regime)
- Dispersion → ~ 23% in V_{pV} between 1 Hz and 500 kHz
- Dispersion decreases with increasing stress

Stress dependence – V_{pV} - Pierre shale

$S_w=0.12$

Frequency (Hz)	Stress sensitivity (m/s/MPa)
1	18.37
500 k	14.30

$S_w=0.27$

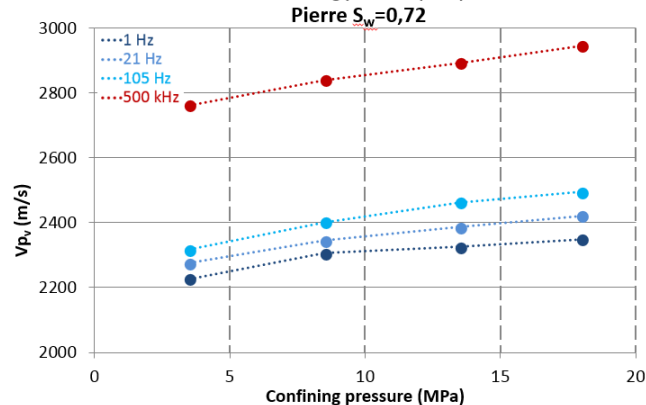
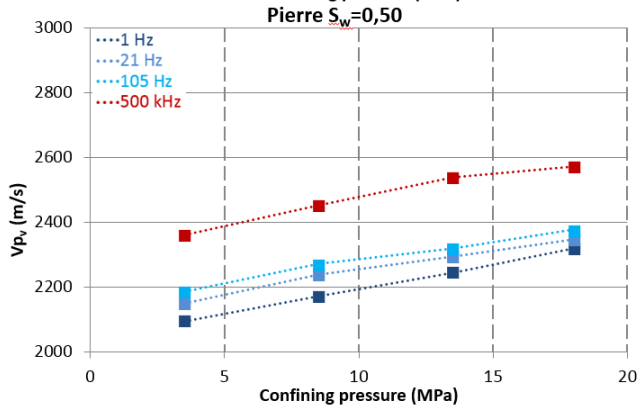
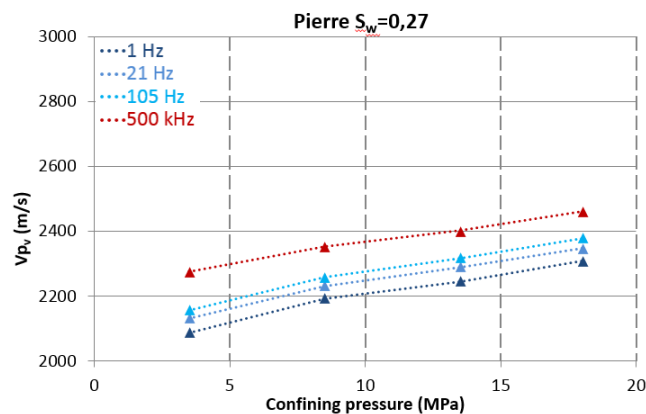
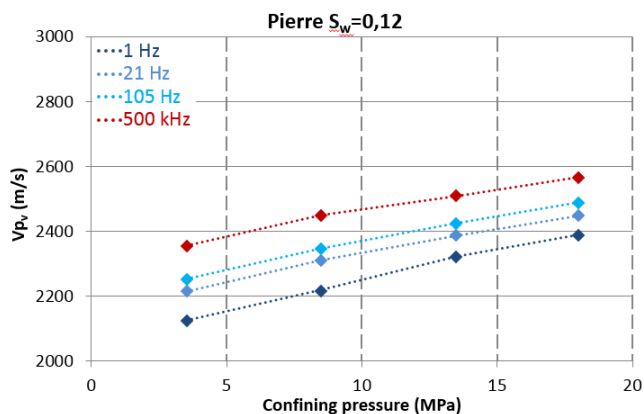
Frequency (Hz)	Stress sensitivity (m/s/MPa)
1	14.76
500 k	12.60

$S_w=0.50$

Frequency (Hz)	Stress sensitivity (m/s/MPa)
1	15.28
500 k	14.95

$S_w=0.72$

Frequency (Hz)	Stress sensitivity (m/s/MPa)
1	7.95
500 k	12.48



- Stress sensitivity → different for seismic and ultrasonic and saturation dependent
- Dispersion → ~ 10% in V_{pV} between 1 Hz and 500 kHz ($S_w=0.12$) and saturation dependent
- Dispersion decreases with increasing stress (beside $S_w=0.72$)
- Effects of saturation increase → stress sensitivity decreases, dispersion increases

Summary

- Absolute E_v changes as a response to hydrostatic loading are similar at seismic and ultrasonic frequencies for both shale types however due to dispersion stress sensitivity is frequency dependent.
- Increase in water saturation level causes increase in E_v dispersion and softening of the shale at seismic frequencies (data not shown in presentation, more in Andreas Bauer talk).
- Stress sensitivity of V_{pV} is frequency dependent (up to twofold decrease from seismic to ultrasonic frequencies) and decreases with the increase of saturation.
- Increase in applied stress decreases dispersion of V_{pV} .
- Increase in water content increases dispersion of V_{pV} .

Acknowledgements

The authors would like to acknowledge support from:

- The BIGCCS program at NTNU and SINTEF.
- The Research Council of Norway.
- The KPN-project “Shale Rock Physics: Improved seismic monitoring for increased recovery” at SINTEF Petroleum Research.

